C. R. Mecanique 344 (2016) 547–555

Contents lists available at ScienceDirect

Comptes Rendus Mecanique

www.sciencedirect.com

Second-law analysis for buoyancy-driven hydromagnetic couple stress fluid flow through a porous channel

Semiu O. Kareem [a,*], Samuel O. Adesanya [b,*], Uchechukwu E. Vincent [a,c]

[a] Department of Physical Sciences, Redeemer's University, Ede, Nigeria
[b] Department of Mathematical Sciences, Redeemer's University, Ede, Nigeria
[c] Department of Physics, Lancaster University, Lancaster LA1 4YB, United Kingdom

ARTICLE INFO

Article history:
Received 19 January 2016
Accepted 10 March 2016
Available online 6 May 2016

Keywords:
Magnetic field
Buoyancy force
Entropy generation
Slip flow
Irreversibility ratio
ADM

ABSTRACT

This paper examines the combined effects of the buoyancy force and of the magnetic field on the entropy generation rate in the flow of a couple stress fluid through a porous vertical channel. The flow's dynamical equations were non-dimensionalised and solved via the application of the Adomian decomposition method (ADM). Variations of some thermo-physical parameters were conducted and discussed, with regard to the physics of the fluid. Our result shows that the entropy generation rate increases as the buoyancy increases in the fluid. In addition, the irreversibility in the flow system results mainly from the fluid's viscosity, ohmic heating, and the buoyancy.

1. Introduction

Over the last few decades, the study of the thermodynamic analysis involving channel fluid flows has attracted a lot of research effort due to its application in several renewable energy systems. Examples of this include the prediction of the efficiency of many thermal systems exchanging heat between two heat reservoirs including other Carnot systems. Basically, the process of energy generation usually culminates in the wastage of excessive energy, which is dissipated in the form of heat. Following from this, there is a need to minimise this inherent wastage by improving the energy of the system. In this regard, few research work had been reported in the literature [1–21]. Specifically, Adesanya and Makinde [1] reported the entropy generation in a couple stress fluid flowing steadily through a porous channel with slip at the isothermal walls, Das et al. [2] examined the entropy generation in a magnetohydrodynamic (MHD) pseudo-plastic nanofluid flow through a porous channel with convective heating. In addition, Adesanya and Makinde [3] studied the entropy generation rate in the couple stress fluid flowing through a porous channel with convective heating at the walls. Eegunjobi and Makinde [4] studied the effect of the buoyancy force and of the Navier slip on the entropy generation rate in a vertical porous channel. The authors also extended their work [5] by investigating the inherent irreversibility of heat transfer in the steady flow of a couple stress fluid through a vertical channel filled with porous materials.

In all the studies in Refs. [1–21] dealing with thermodynamic analysis linked with channel fluid flow, the combined effect of a uniform magnetic field applied transversely to the flow channel and the buoyancy force due to a change in the temperatures at the two boundary plates were neglected. However, magnetohydrodynamics (MHD) fluid flow, which is

* Corresponding authors.
E-mail addresses: kareems@run.edu.ng (S.O. Kareem), adesanyas@run.edu.ng (S.O. Adesanya), u.vincent@lancaster.ac.uk (U.E. Vincent).

http://dx.doi.org/10.1016/j.crme.2016.03.003
1631-0721/

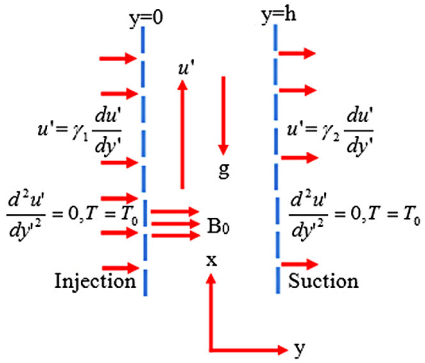

Fig. 1. The geometry of the model.

partly dependent on buoyancy, plays a vital role in many industrial and thermal engineering applications. For instance, it is useful in controlled irrigation systems, controlling extremely hot moving fluids like molten steel and liquid film, as well as in the polymer industry. Many researchers have examined the entropy analysis in a buoyancy-driven fluid flow. For example, Riley [22] presented a buoyancy-dependent MHD flow. Also, Alboussière et al. [23] investigated the asymptotic behaviour of a buoyancy-driven convection in the presence of a uniform magnetic field. Moreover, Eegunjobi and Makinde in [4,5] examined the second-law analysis for a buoyancy-driven incompressible fluid flow through a porous channel by imposing Navier slip conditions at the walls. In the same vein, Makinde and Chinyoka [24] examined the inherent irreversibility for flow and heat transfer inside a vertical channel made of two uniformly porous parallel plates with suction/injection under the combined action of a buoyancy force, a transverse magnetic field, and a constant pressure gradient.

Motivated by studies in [4,5,22–25], the objective of the present study is to examine the combined influence of the buoyancy and the magnetic field of the couple stress fluid on entropy generation within the flow channel, which has not been accounted for in the previous studies. The outcoming results are expected to enhance many industrial and thermal engineering processes whose working medium is a non-Newtonian fluid, with a view to minimise entropy generation, which tends to deplete the amount of useful energy for work.

To achieve this objective, flow-governing equations are formulated, non-dimensionalised, and approximate solutions to the dimensionless coupled non-linear boundary-value problem are obtained by using a semi-analytical Adomian decomposition method [26,27]. This method has been chosen because it does not require any linearisation, discretisation, use of initial guess or pertubation. These approximation solutions are used to compute the entropy generation rate and the irreversibility ratio.

In the following section, the problem is formulated, and a non-dimensional analysis is also presented. Section 3 contains the problem-solving method, the results are presented and discussed in Section 4, while Section 5 concludes the paper.

2. Mathematical formulation

A steady hydromagnetic non-Newtonian fluid flow between two permeable parallel vertical plates, with upthrust effect, is considered. The parallel plates are stationary regarding the motion of the fluid, as shown in the geometry of the problem (see Fig. 1). A 2-dimensional perpendicular coordinate system is employed, with the x-axis along the flow direction for the problem analysis. The width of the channel is $y = h$. Fluid injection occurs at the plate, where $y = 0$ at a uniform rate v_0. The system also allows fluid suction at the plate where $y = h$, at the same velocity v_0. A constant magnetic field of strength B_0 is applied perpendicular to the direction of the fluid flow. The flow problem is analysed so that no external voltage is applied to the flow system, and with negligible induced magnetic field and Hall effect. With reference to Boussinesq's approximation [28], a density difference exists in the flow system due to the temperature difference at the isothermal walls, which results in the buoyancy force contribution in the constitutive system equations. From this, the momentum and energy balance equations, with the local volumetric entropy generation rate (E_G) for the fluid flow, can be written as follows [1,4,12]:

$$v_0 \rho \frac{\mathrm{d}u'}{\mathrm{d}y'} = -\frac{\mathrm{d}P}{\mathrm{d}x'} + \mu \frac{\mathrm{d}^2u'}{\mathrm{d}y'^2} - \eta \frac{\mathrm{d}^4u'}{\mathrm{d}y'^4} - \sigma_e B_0^2 u' + g\beta(T - T_0) \tag{1}$$

$$\rho c_P v_0 \frac{\mathrm{d}T}{\mathrm{d}y'} = \kappa \frac{\mathrm{d}^2T}{\mathrm{d}y'^2} + \mu \left(\frac{\mathrm{d}u'}{\mathrm{d}y'}\right)^2 + \eta \left(\frac{\mathrm{d}^2u'}{\mathrm{d}y'^2}\right)^2 + \sigma_e B_0^2 u'^2 \tag{2}$$

$$E_G = \frac{\kappa}{T_0^2}\left(\frac{\mathrm{d}T}{\mathrm{d}y'}\right)^2 + \frac{\mu}{T_0}\left(\frac{\mathrm{d}u'}{\mathrm{d}y'}\right)^2 + \frac{\eta}{T_0}\left(\frac{\mathrm{d}^2u'}{\mathrm{d}y'^2}\right)^2 + \frac{\sigma_e}{T_0} B_0^2 u'^2 \tag{3}$$

In this present analysis, the extended Navier boundary condition is used. Therefore, the appropriate boundary condition for the flow system may be written as

$$u'(0) = \gamma_1 \frac{\mathrm{d}u'(0)}{\mathrm{d}y'} - \frac{\alpha\eta}{\mu}\frac{\mathrm{d}^3u'(0)}{\mathrm{d}y'^3}, \frac{\mathrm{d}^2u'(0)}{\mathrm{d}y'^2} = 0, T(0) = T_0 \tag{4}$$

$$u'(1) = \gamma_2 \frac{\mathrm{d}u'(1)}{\mathrm{d}y'} - \frac{\alpha\eta}{\mu}\frac{\mathrm{d}^3u'(1)}{\mathrm{d}y'^3}, \frac{\mathrm{d}^2u'(1)}{\mathrm{d}y'^2} = 0, T(1) = T_0 \tag{5}$$

where u' and P are the fluid velocity and pressure respectively, v_0 is the injection/suction velocity at the channel walls, η is the coefficient of the couple stress, μ is the dynamic viscosity, γ_i corresponds to the Navier slip coefficients at the lower and upper plates, respectively for $i = 1, 2$, ρ is the fluid density, σ_e is the fluid electrical conductivity, κ is the coefficient of thermal conductivity, c_P is the isobaric specific heat, T_f and T_0 are the final and initial fluid temperatures, respectively, T is the temperature of the fluid, β is the volumetric expansion coefficient, g is the acceleration due to gravity and $\alpha = 1$ is a variable constant.

In Eq. (1), the applied magnetic field B of magnitude B_0 may be analysed using the following Maxwell's equations and Ohm's law:

$$\nabla.B = 0, \nabla \times B = \mu_\mathrm{m} J, J = \sigma_\mathrm{e}(E + u' \times B) \tag{6}$$

where μ_m is the magnetic permeability, J is the current density, u' is the fluid velocity, σ_e is the fluid electrical conductivity, and E is the fluid electrical field. We consider a flow system with a small induced magnetic field, hence $\mu_\mathrm{m} = 0$. In addition, there is no applied voltage or polarisation voltage in the flow system, hence $E = 0$. The effective electromagnetic force in the fluid may be defined as:

$$E_\mathrm{m} = J \times B \tag{7}$$

Using Eq. (6) in Eq. (7):

$$E_\mathrm{m} = -\sigma_\mathrm{e} u' B_0^2 \hat{i} \tag{8}$$

where $\hat{i}$ is a unit vector in the x-direction.

Using the following dimensionless parameters and variables in Eqs. (1)–(5):

$$y = \frac{y'}{h}, u = \frac{u'}{v_0}, \theta = \frac{T - T_0}{T_\mathrm{f} - T_0}, s = \frac{v_0 h}{\nu}, G = -\frac{h^2}{\mu v_0}\frac{\mathrm{d}P}{\mathrm{d}x'}$$
$$a^2 = \frac{\mu h^2}{\eta}, Ha^2 = \frac{\sigma_\mathrm{e} h^2 B_0^2}{\mu}, Pr = \frac{\nu \rho c_P}{\kappa}, Br = \frac{v_0^2 \mu}{\kappa(T_f - T_0)}$$
$$\Omega = \frac{T_\mathrm{f} - T_0}{T_0}, Gr = \frac{g\beta h^2(T_\mathrm{f} - T_0)}{\mu v_0}, N_s = \frac{T_0^2 h^2 E_\mathrm{G}}{\kappa(T_\mathrm{f} - T_0)^2}$$
$$\beta_1 = \frac{\gamma_1}{h}, \beta_2 = \frac{\gamma_2}{h} \tag{9}$$

Eqs. (1)–(3) may be written in the form of dimensionless boundary value problems, as

$$s\frac{\mathrm{d}u}{\mathrm{d}y} = G + \frac{\mathrm{d}^2u}{\mathrm{d}y^2} - \frac{1}{a^2}\frac{\mathrm{d}^4u}{\mathrm{d}y^4} - Ha^2u + Gr\theta \tag{10}$$

$$sPr\frac{\mathrm{d}\theta}{\mathrm{d}y} = sPr\frac{\mathrm{d}\theta}{\mathrm{d}y} = \frac{\mathrm{d}^2\theta}{\mathrm{d}y^2} + Br(\frac{\mathrm{d}u}{\mathrm{d}y})^2 + \frac{Br}{a^2}(\frac{\mathrm{d}^2u}{\mathrm{d}y^2})^2 + BrHa^2u^2 \tag{11}$$

together with the boundary conditions

$$u(0) = \beta_1(\frac{\mathrm{d}u(0)}{\mathrm{d}y} - \frac{\alpha}{a^2}\frac{\mathrm{d}^3u(0)}{\mathrm{d}y^3}), \frac{\mathrm{d}^2u(0)}{\mathrm{d}y^2} = 0, \theta(0) = 0$$
$$u(1) = \beta_2(\frac{\mathrm{d}u(1)}{\mathrm{d}y} - \frac{\alpha}{a^2}\frac{\mathrm{d}^3u(1)}{\mathrm{d}y^3}), \frac{\mathrm{d}^2u(1)}{\mathrm{d}y^2} = 0, \theta(1) = 0 \tag{12}$$

while the entropy generation can be computed using

$$N_s = (\frac{\mathrm{d}\theta}{\mathrm{d}y})^2 + \frac{Br}{\Omega}(\frac{\mathrm{d}u}{\mathrm{d}y})^2 + \frac{Br}{\Omega a^2}(\frac{\mathrm{d}^2u}{\mathrm{d}y^2})^2 + \frac{Br}{\Omega}Ha^2u^2 \tag{13}$$

The present model – Eqs. (1), (2) and (3) – is comparable to that studied by Adesanya and Makinde [1] in the asymptotic case corresponding to $Ha^2, Gr, \alpha \to 0$, and Eegunjobi and Makinde [4] in the asymptotic case where $Ha^2, \eta, \alpha \to 0$.

3. Adomian decomposition method of solution

In this section, the semi-analytical Adomian decomposition method is employed to obtain the solutions to the momentum equation (10), the energy equation (11), and the entropy production equation (13), subjected to boundary condition (12). Usually, the boundary value problems are converted into the equivalent integral equations with $u''(0) = u''(1) = 0$. Thus,

$$u(y) = f_0 + \int_0^y f_1 \,\mathrm{d}Y + \int_0^y \int_0^y \int_0^y f_2 \mathrm{d}Y\mathrm{d}Y\mathrm{d}Y + a^2 \int_0^y \int_0^y \int_0^y \int_0^y F_4(Y)\,\mathrm{d}Y\mathrm{d}Y\mathrm{d}Y\mathrm{d}Y \tag{14}$$

$$\theta(y) = c_0 + c_1\, y + \int_0^y \int_0^y \left(F_2(Y) - BrHa^2u^2\right)\mathrm{d}Y\mathrm{d}Y \tag{15}$$

where

$$f_0 = u(0),$$
$$f_1 = \left(\frac{\mathrm{d}u}{\mathrm{d}y}|_{y=0}\right)$$
$$f_2 = \left(\frac{\mathrm{d}^3u}{\mathrm{d}y^3}|_{y=0}\right)$$
$$F_4(Y) = G + \frac{\mathrm{d}^2u}{\mathrm{d}Y^2} - s\frac{\mathrm{d}u}{\mathrm{d}Y} - Ha^2u + Gr\theta$$
$$F_2(Y) = sPr\frac{\mathrm{d}\theta}{\mathrm{d}Y} - Br\left(\frac{\mathrm{d}u}{\mathrm{d}Y}\right)^2 - \frac{Br}{a^2}\left(\frac{\mathrm{d}^2u}{\mathrm{d}Y^2}\right)^2$$

The coefficients f_0, f_1, f_2, c_0 and c_1 in Eqs. (14), (15) were determined by using the method of undetermined coefficients. Next, the flow velocity is considered to be in form of the infinite series:

$$u(y) = \sum_0^\infty u_n(y), \theta(y) = \sum_0^\infty \theta_n(y) \tag{16}$$

Substituting (16) into (14) and (15), we obtain:

$$\sum_{n=0}^{n=\infty} u_n(y) = f_0 + f_1 y + \frac{y^3}{6} f_2 + a^2 L_4(Y)\,\mathrm{d}Y\mathrm{d}Y\mathrm{d}Y\mathrm{d}Y \tag{17}$$

and

$$\sum_{n=0}^{n=\infty} \theta_n(y) = c_0 + c_1 y + \int_0^y \int_0^y \left(Z_1 - Z_2\right)\mathrm{d}Y\mathrm{d}Y \tag{18}$$

where

$$L_4(Y) = \int_0^y \int_0^y \int_0^y \int_0^y \left(G + \sum_{n=0}^{n=\infty} \frac{\mathrm{d}^2u_n}{\mathrm{d}Y^2} - s\sum_{n=0}^{n=\infty} \frac{\mathrm{d}u_n}{\mathrm{d}Y} - Ha^2 \sum_{n=0}^{n=\infty} u_n\right)$$

$$S_1 = sPr \sum_{n=0}^{n=\infty} \frac{\mathrm{d}\theta_n}{\mathrm{d}Y} - Br \sum_{n=0}^{n=\infty} \left(\frac{\mathrm{d}u_n}{\mathrm{d}Y}\right)^2$$

and

$$S_2 = \frac{Br}{a^2} \sum_{n=0}^{n=\infty} \left(\frac{\mathrm{d}^2u_n}{\mathrm{d}Y^2}\right)^2 - BrHa^2 \sum_{n=0}^{n=\infty} u_n^2$$

Following from the above, (16) may be expressed in the recursive form

$$u_0(y) = f_0 + f_1 y + \frac{y^3}{6} f_2 + a^2 \int_0^y \int_0^y \int_0^y \int_0^y G \, \mathrm{d}Y \mathrm{d}Y \mathrm{d}Y \mathrm{d}Y \tag{19}$$

$$u_{n+1}(y) = a^2 \int_0^y \int_0^y \left(\frac{\mathrm{d}^2 u_n}{\mathrm{d}Y^2} - s \frac{\mathrm{d}u_n}{\mathrm{d}Y} - Ha^2 u_n + Gr\theta \right) \mathrm{d}Y \mathrm{d}Y \tag{20}$$

To further simplify the computational task with a view to reducing the computational load in (18), the modified recurrent relation

$$\theta_0(y) = c_1 y \tag{21}$$

is used, so that

$$\theta_1(y) = \int_0^y \int_0^y \left(sPr \sum_{n=0}^{n=\infty} \frac{\mathrm{d}\theta_0}{\mathrm{d}Y} - \frac{Br}{a^2} \left(\frac{\mathrm{d}^2 u}{\mathrm{d}Y^2} \right)^2 \right) \mathrm{d}Y \mathrm{d}Y \tag{22}$$

$$\theta_2(y) = \int_0^y \int_0^y \left(sPr \sum_{n=0}^{n=\infty} \frac{\mathrm{d}\theta_1}{\mathrm{d}Y} - Br \left(\frac{\mathrm{d}u}{\mathrm{d}Y} \right)^2 \right) \mathrm{d}Y \mathrm{d}Y \tag{23}$$

$$\theta_3(y) = \int_0^y \int_0^y \left(sPr \sum_{n=0}^{n=\infty} \left(\frac{\mathrm{d}\theta_2}{\mathrm{d}Y} - BrHa^2 u^2 \right) \right) \mathrm{d}Y \mathrm{d}Y \tag{24}$$

$$\theta_{n+1}(y) = \int_0^y \int_0^y \left(sPr \sum_{n=0}^{n=\infty} \frac{\mathrm{d}\theta_n}{\mathrm{d}Y} \right) \mathrm{d}Y \mathrm{d}Y; \quad (n \geq 2) \tag{25}$$

It has been shown in [8] that the ADM series solution converges rapidly. As a result, few terms of the series can guarantee reliable approximate solutions to the problem. Here, we set the number of iterations to $m = 3$, so that the approximate solutions (16) may be written as finite series as follows:

$$u(y) = \sum_0^3 u_n(y), \theta(y) = \sum_0^3 \theta_n(y) \tag{26}$$

The irreversibility in the heat flow to the viscous fluid is analysed using (13) by expressing the entropy generation number N_s as a partial sum of the entropy generation due to heat transfer, and the irreversibility resulting from fluid friction and Ohmic heating of the fluid. Therefore we set N_1 and N_2 as follows:

$$N_1 = \left(\frac{\mathrm{d}\theta}{\mathrm{d}y} \right)^2, N_2 = \frac{Br}{\Omega} \left(\frac{\mathrm{d}u}{\mathrm{d}y} \right)^2 + \frac{Br}{\Omega a^2} \left(\frac{\mathrm{d}^2 u}{\mathrm{d}y^2} \right)^2 + \frac{Br}{\Omega} Ha^2 u^2 \tag{27}$$

The Bejan number *Be*, which is a parameter that measures the irreversibility ratio in the heat flow, may be defined as

$$Be = \frac{N_1}{N_s} = \frac{1}{1 + \Phi}, \Phi = \frac{N_2}{N_1} \tag{28}$$

where Φ is the irreversibility ratio, a parameter that measures the rate of destruction of the available work in the flow system. The Bejan number in Eq. (28) is bounded in the interval $0 \leq Be \leq 1$. The irreversibility due to heat transfer is dominant when $Be = 1$, while the irreversibility due to viscosity and magnetic field is dominant when $Be = 0$. The dimensionless equations (10)–(13), with the boundary conditions (12), were solved using the algorithm in (19)–(26), coded in MATHEMATICA symbolic package. Using the numerical procedure discussed above, we computed the dimensionless velocity, temperature, entropy generation, and irreversibility ratio. In what follows, we discussed some interesting results from our findings.

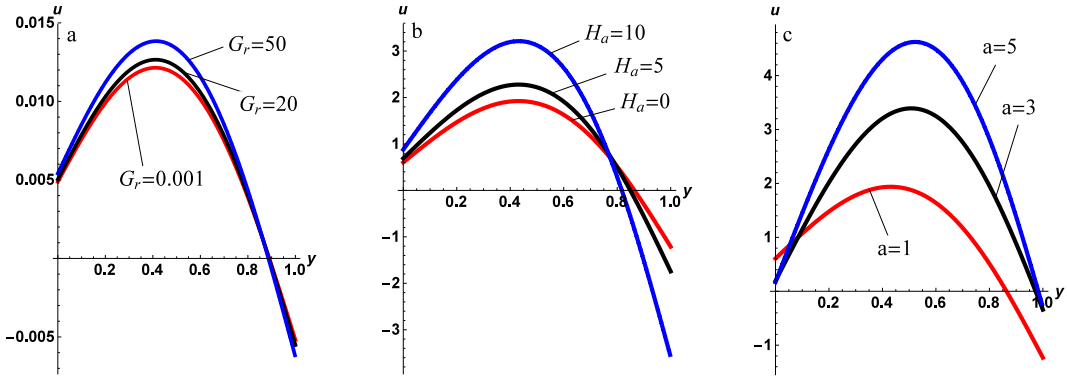

Fig. 2. Parameterised velocity profiles of the fluid flow: (a) by varying the Grashof number Gr, with $Ha = 1$, $Br = 5$, $Pr = 25$, $\Omega = 1$, $a = s = 1$, $\beta_1 = \beta_2 = 0.1$; (b) by varying the Hartmann number Ha, with $Gr = 1$, $Br = 5$, $Pr = 25$, $\Omega = 1$, $a = s = 1$, $\beta_1 = \beta_2 = 0.1$; (c) by varying the couple stress inverse a, with $Gr = 1$, $Ha = 1$, $Br = 5$, $Pr = 25$, $\Omega = 1$, $s = 1$, $\beta_1 = \beta_2 = 0.1$.

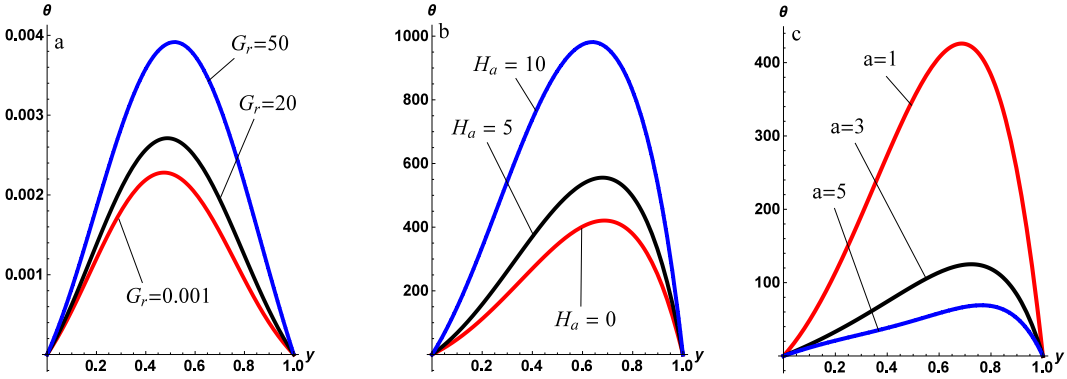

Fig. 3. Parameterised temperature profiles of the fluid flow: (a) by varying the Grashof number Gr, with $Ha = 1$, $Br = 5$, $Pr = 25$, $\Omega = 1$, $a = s = 1$, $\beta_1 = \beta_2 = 0.1$; (b) by varying the Hartmann number Ha, with $Gr = 1$, $Br = 5$, $Pr = 25$, $\Omega = 1$, $a = s = 1$, $\beta_1 = \beta_2 = 0.1$; (c) by varying the couple stress inverse a, with $Gr = 1$, $Ha = 1$, $Br = 5$, $Pr = 25$, $\Omega = 1$, $s = 1$, $\beta_1 = \beta_2 = 0.1$.

4. Results and discussion

We start by examining the effect of a number of parameters in the dimensionless model equations, which govern, in this present paper, the evolution of the fluid velocity u, of the fluid temperature θ, of the entropy generation N_S, and of the irreversibility ratio Be. These are the Grashof number, Gr, the Hartmann number Ha, and the couple stress inverse parameter a. In Fig. 2a, we investigate the effect of buoyancy, in terms of Gr, on the flow velocity, with respect to the width of the flow channel. It is observed from this figure that as Gr increases, the fluid momentum also increases. As a result, the flow velocity increases. The buoyancy effect is gravity and temperature difference dependent. The buoyancy effect is not significant at the walls. In Fig. 2b, the applied magnetic field showed the same behaviour as the buoyancy effect as regards the evolution of the flow velocity profile. As the Hartmann number, Ha, increases, the fluid particles speed up mainly at the centreline of the flow channel. The Lorentz force constitutes the resistance/drag to the flow of electrically conducting fluid, which effectively reduces the momentum of the fluid parcels in the adjacent fluid layers. In contrast, our study shows that the velocity of the flow increases as the strength of the magnetic field increases. This is due to the presence of buoyancy forces in the flow system. As the fluid surges, the effective positive jump in the velocity of the fluid parcels suppresses the decreasing rate of change of momentum caused by the Lorentz force in the flow system, thereby increasing the velocity of the fluid. Fig. 2c shows the effect of increasing the couple stress inverse parameter on the velocity of the flow. It is observed from the figure that increasing the couple stress inverse parameter also increases the velocity of the fluid motion. This is caused by the reduction in the friction arising from the effect of particle additives, which constitute a size-dependent effect in couple stress fluids. Moreover, the rotational field of the fluid particles becomes minimal. Consequently, an increase in the couple stress results in a corresponding increase in the velocity profile of the fluid.

Also in Fig. 3, the behaviour of the flow temperature is described with respect to the buoyancy effect, the magnetic field parameter, and the couple stress inverse parameter. It is clear from Fig. 3a that increasing the Grashof number, Gr, increases the temperature of the fluid. This can be explained by the increase in the translational kinetic energy of the flow. Buoyancy increases the fluid velocity. As a result, the kinetic energy, $E = \frac{1}{2}mu^2$ (in terms of the fluid particle's mass m and velocity u) increases, resulting in an increase in the fluid's thermodynamic temperature. The kinetic energy E is comparable with the Brinkman number given by $Br = \frac{1}{2}mv_0^2$, where $m = \frac{2\mu}{\kappa(T_f - T_0)}$. It is observed in Fig. 3b that the increase in the magnetic

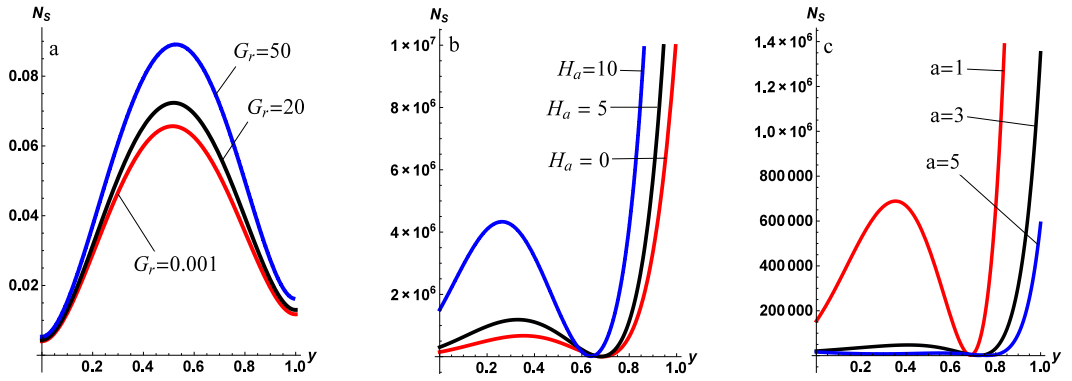

Fig. 4. Entropy generation rate: (a) by varying the Grashof number Gr, with $Ha = 1$, $Br = 5$, $Pr = 25$, $\Omega = 1$, $a = s = 1$, $\beta_1 = \beta_2 = 0.1$; (b) by varying the Hartmann number Ha with $Gr = 1$, $Br = 5$, $Pr = 25$, $\Omega = 1$, $a = s = 1$, $\beta_1 = \beta_2 = 0.1$; (c) by varying the couple stress inverse a, with $Gr = 1$, $Ha = 1$, $Br = 5$, $Pr = 25$, $\Omega = 1$, $s = 1$, $\beta_1 = \beta_2 = 0.1$.

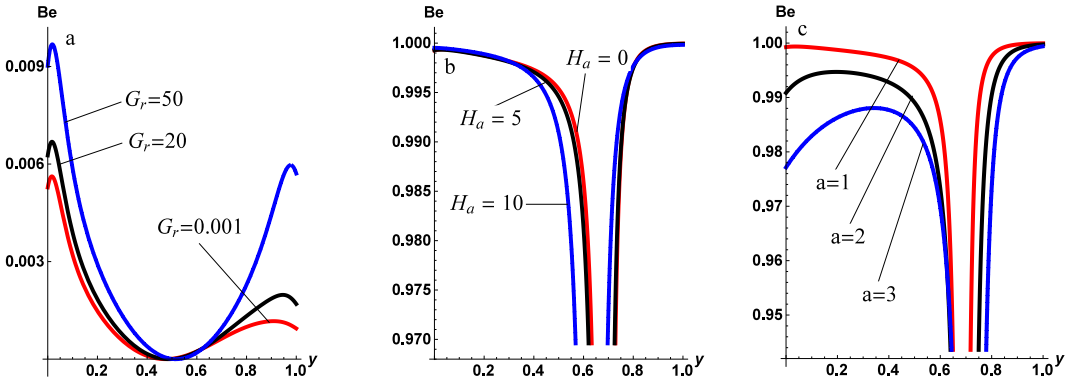

Fig. 5. Irreversibility ratio: (a) by varying the Grashof number Gr, with $Ha = 1$, $Br = 5$, $Pr = 25$, $\Omega = 1$, $a = s = 1$, $\beta_1 = \beta_2 = 0.1$; (b) by varying the Hartmann number Ha, with $Gr = 1$, $Br = 5$, $Pr = 25$, $\Omega = 1$, $a = s = 1$, $\beta_1 = \beta_2 = 0.1$; (c) by varying the couple stress inverse a, with $Gr = 1$, $Ha = 1$, $Br = 5$, $Pr = 25$, $\Omega = 1$, $s = 1$, $\beta_1 = \beta_2 = 0.1$.

field intensity results in an increase in the channel's temperature, while Fig. 3c reveals that increasing the couple stresses decreases the temperature profile in the channel. Expectedly, couple stresses enhance the fluid's intermolecular cohesion, thereby increasing the fluid's resistance to shear stress; consequently, the temperature rises within the flow channel.

Furthermore, entropy production shows an interesting response to changes in buoyancy, as revealed by Fig. 4a. The fluid shows an increasing degree of randomness in the fluid particles, mainly at the centreline of the channel, as the Grashof number increases. The increased randomness here is due to the increased rate of change of momentum in the fluid as the parameter Gr increases. This is also observed in Fig. 4b. Entropy generation increases as the magnetic field strength increases, but with entropy freeze-out in the width region $0.64 \leq y \leq 0.68$. Moreover, in Fig. 4c, a reversed scenario is observed. The rate of entropy generation decreases rapidly as the couple stress inverse parameter increases.

Fig. 5 shows the dominance of the two forms of irreversibilities inherent to the fluid, namely the irreversibility due to fluid viscosity, ohmic heating, and buoyancy, and irreversibility due to heat transfer. We refer to the Bejan number versus the channel's width (Be–y) chart as Entropy Contribution to Irreversibility Scale (ECIS), which compares the partial irreversibilities contributed by the different entropy sources such as N_1 and N_2 to the total irreversibility in the flow system. It is clear from Fig. 5a that, as Gr increases, the irreversibility due to fluid viscosity, Joule heating, and buoyancy dominates. In Fig. 5b and c, it is observed that as the Hartmann number Ha and the couple stress inverse parameter a increase, the irreversibility due to heat transfer dominates.

5. Conclusion

In this work, we examined the combined effect of buoyancy and magnetic field on the entropy generation in a couple stress hydromagnetic fluid flow, using the Adomian decomposition method to obtain the analytical solution that approximates the velocity and temperature profiles, which are used to obtain the entropy generation production as well as the Bejan number. We observed that the addition of the buoyancy force into the momentum balance equation reveals a rather interesting channel fluid flow dynamics. Buoyancy could enhance the fluid velocity response as well as the temperature of the system. We showed that an increase in buoyancy forces results in a regime of irreversibility ratio dominated by the irreversibility due to fluid viscosity, ohmic heating, and buoyancy. In addition, it was found that the entropy generation rate increases with increasing buoyancy forces.

Nomenclature

u	dimensionless fluid velocity	x', y'	Cartesian coordinates
s	suction/injection parameter	x, y	dimensionless Cartesian coordinates
Pr	Prandtl number	B_0	magnetic field strength
Br	Brinkman number	μ	dynamic viscosity
Gr	Grashof number	σ_e	electrical conductivity
a^2	couple stress parameter	η	coefficient of couple stress
Ω	parameter that measures the temperature difference between the two heat reservoirs	u'	fluid velocity
		E_G	volumetic rate of entropy
G	dimensionless pressure gradient	N_s	entropy generation number
β_1	dimensionless Navier slip parameter at the lower wall	N_1	entropy generation due to heat transfer
		N_2	entropy generation due to entropy generation due to fluid friction and ohmic heating
β_2	dimensionless Navier slip parameter at the upper wall		
Ha^2	Hartmann number	κ	thermal conductivity
T	fluid temperature	ρ	fluid density
T_f	final fluid temperature	c_P	specific heat at constant pressure
γ_1	Navier slip coefficient at the lower plate	T_0	temperature at the lower plate
γ_2	Navier slip coefficient at the upper plate	θ	dimensionless fluid temperature
v_0	uniform suction/injection velocity	β	volumetric expansion coefficient
h	width of the channel	g	acceleration due to gravity

Acknowledgements

UEV is supported by the Royal Society of London, through their Newton International Fellowship Alumni scheme.

References

[1] S.O. Adesanya, O.D. Makinde, Entropy generation in couple stress fluid flow through porous channel with fluid slippage, Exergy 15 (3) (2014) 344–362.
[2] S. Das, A.S. Banu, R.N. Jana, O.D. Makinde, Entropy analysis on MHD pseudo-plastic nanofluid flow through a vertical porous channel with convective heating, Alex. Eng. J. 54 (3) (2015) 325–337.
[3] S.O. Adesanya, O.D. Makinde, Effects of couple stresses on entropy generation rate in a porous channel with convective heating, Comput. Appl. Math. 34 (2015) 293–307.
[4] A.S. Eegunjobi, O.D. Makinde, Combined effect of buoyancy force and Navier slip on entropy generation in a vertical porous channel, Entropy 14 (2012) 1028–1044.
[5] O.D. Makinde, A.S. Eegunjobi, Entropy generation in a couple stress fluid flow through a vertical channel filled with saturated porous media, Entropy 15 (11) (2013) 4589–4606.
[6] J.A. Esfahani, M. Modirkhazeni, Entropy generation of forced convection film condensation on a horizontal elliptical tube, C. R. Mecanique 340 (7) (2012) 543–551.
[7] Y. Wang, Z. Chen, X. Ling, Entropy generation analysis of particle suspension induced by Couette flow, Int. J. Heat Mass Transf. 90 (2015) 499–504.
[8] S.O. Adesanya, O.D. Makinde, Thermodynamic analysis for a third grade fluid through a vertical channel with internal heat generation, J. Hydrodyn. 27 (2) (2015) 264–272.
[9] S.O. Adesanya, O.D. Makinde, Irreversibility analysis in a couple stress film flow along an inclined heated plate with adiabatic free surface, Physica A 432 (2015) 222–229.
[10] S.O. Adesanya, S.O. Kareem, J.A. Falade, S.A. Arekete, Entropy generation analysis for a reactive couple stress fluid flow through a channel saturated with porous material, Energy 93 (1) (2015) 1239–1245.
[11] S.O. Adesanya, J.A. Falade, Thermodynamics analysis of hydromagnetic third grade fluid flow through a channel filled with porous medium, Alex. Eng. J. 54 (3) (2015) 615–622.
[12] S. Das, R.N. Jana, Effect of hall current on entropy generation in porous channel with suction/injection, Int. J. Energy Technol. 5 (25) (2013) 1–11.
[13] C.K. Chen, B.S. Chen, C.C. Liu, Entropy generation in mixed convection magnetohydrodynamic nanofluid flow in vertical channel, Int. J. Heat Mass Transf. 91 (2015) 1026–1033.
[14] N. Saeid, Magnetic field effects on entropy generation in heat and mass transfer in porous cavity, Acad. J. 8 (17) (2013) 728–739.
[15] M. Magherbi, A. El-Jery, N. Hidouri, A.B. Brahim, Evanescent magnetic field effects on entropy generation at the on set of natural convection, Indian Acad. J. 35 (2) (2010) 163–176.
[16] A. El-Jery, N. Hidouri, M. Magherbi, A.B. Brahim, Effect of external oriented magnetic field on entropy generation in natural convection, Entropy 12 (2010) 1391–1417.
[17] S. Salas, S. Cuevas, M.L. Haro, Entropy analysis of magnetohydrodynamic induction devices, J. Phys. D, Appl. Phys. 32 (1999) 2605–2608.
[18] S.H. Tasnim, M.A.H. Mahmud, Entropy generation in a porous channel with hydromagnetic effects, Exergy 2 (2002) 300–308.
[19] S. Mahmud, S.H. Tasnim, H.A.A. Mamun, Thermodynamics analysis of mixed convection in a channel with transverse hydromagnetic effect, Int. J. Therm. Sci. 42 (731–740) (2003).
[20] D. Theuri, O.D. Makinde, Themodynamic analysis of variable viscosity MHD unsteady generalized Coutte flow with permeable walls, Appl. Comput. Math. 3 (1) (2014) 1–8.
[21] O. Mahian, H.F. Oztop, I. Pop, S. Mahmud, S. Wongwises, Design of vertical annulus with MHD flow using entropy generation analysis, Therm. Sci. 17 (4) (2013) 1013–1022.
[22] N. Riley, Magnetohydrodynamics free convection, J. Fluid Mech. 18 (1964) 577–586.

[23] T. Alboussière, J.P. Garandet, R. Moreau, Buoyancy-driven convection with a uniform magnetic field, part 1: asymptotic analysis, J. Fluid Mech. 253 (1983) 545–563.
[24] O.D. Makinde, T. Chinyoka, Numerical investigation of buoyancy effects on hydromagnetic unsteady flow through a porous channel with suction/injection, J. Mech. Sci. Technol. 27 (5) (2013) 1557–1568.
[25] K. Kaladhar, Natural convection flow of couple stress fluid in vertical channel with hall and Joule effects, Proc. Eng. 127 (2015) 1071–1078.
[26] G. Adomian, Solving Frontier Problems of Physics: The Decomposition Method, Kluwer Academic Publishers, Dordrecht, 1994.
[27] J.S. Duan, R. Rach, A new modification of the Adomian decomposition method for solving boundary value problems for higher order nonlinear differential equations, Appl. Math. Comput. 218 (2011) 4090–4118.
[28] W.M. Macek, M. Strumik, Model for hydromagnetic convection in a magnetized fluid, Phys. Rev. E 82 (4) (2010) 027301.